

Research article***Chromolaena odorata* Extract as an Eco-Friendly Reducing Agent for Graphene Oxide**

Watsayod Ananpreechakorn^{1,2}, Krittaphat Wongma¹, Theerawut Sumpaho², Sunti Phewphong², Nattawat Anuwongsa³ and Hassakorn Wattanasarn^{2,3*}

¹*Program of Science, Faculty of Education, Sakon Nakhon Rajabhat University, Sakon Nakhon, Thailand*

²*Center of Excellence on Alternative Energy, Research and Development Institute, Sakon Nakhon Rajabhat University, Sakon Nakhon, Thailand*

³*Program of Physics, Faculty of Science and Technology, Sakon Nakhon Rajabhat University, Sakon Nakhon, Thailand*

Received: 8 March 2024, Revised: 29 July 2024, Accepted: 7 October 2024, Published: 15 November 2024

Abstract

Chromolaena odorata (Siam weed) was researched for its application as a novel reducing agent. Graphene oxide (GO) was prepared via a modified Hummers method, and its reduction was achieved using an aqueous extract of *Chromolaena odorata* leaves. The use of conventional reducing agents typically results in hydrophobic reduced graphene oxide (rGO), which leads to agglomeration in solvents. However, the green reduction method using *Chromolaena odorata* extract achieved a homogeneous dispersion, which is crucial for applications requiring simple preparation techniques such as magnetic stirring, ultrasonic sonication, and vacuum mixing. Characterization of the rGO revealed a broad peak around 24.12° in the x-ray diffraction (XRD) pattern, an increased I_D / I_G ratio of 1.09 from Raman spectroscopy, and a high C:O ratio of 5.07 from energy dispersive x-ray spectroscopy (EDS). Additionally, BET analysis demonstrated an increase in surface area and pore volume, while FESEM analyses showed a uniform morphology with clear structural defects and minimal oxygen content. FTIR spectra further confirmed the reduction process, indicated significant decrease in oxygen-related peaks. These findings highlight the potential of *Chromolaena odorata* as a sustainable reducing agent for the environmentally friendly synthesis of high-quality rGO.

Keywords: *Chromolaena odorata*; reduced graphene oxide; eco-friendly; invasive plant; green synthesis

*Corresponding author: E-mail: w_hussakorn@snru.ac.th

<https://doi.org/10.55003/cast.2024.262140>

Copyright © 2024 by King Mongkut's Institute of Technology Ladkrabang, Thailand. This is an open access article under the CC BY-NC-ND license (<http://creativecommons.org/licenses/by-nc-nd/4.0/>).

1. Introduction

The exploration of graphene, a monolayer of carbon atoms that form a two-dimensional honeycomb lattice was a crucial advance in the field of materials science. Its exceptional properties include its electrical conductivity and its charge carrier mobility at room temperature of up to $10,000 \text{ cm}^2 \text{ V}^{-1} \text{ s}^{-1}$ (Alwan et al., 2023). Based on the degree of reduction and restoration of the sp^2 hybridized carbon network (Pei et al., 2012), the surface area range widely, typically between 500 to 1500 $\text{m}^2 \text{ g}^{-1}$, depending on the synthesis method and the degree of reduction (Zhu et al., 2010). Thermal conductivity values in the range of 500 to 1,500 $\text{W m}^{-1} \text{ K}^{-1}$, though this can be influenced by the quality of the rGO, its layer structure, and the presence of defects (Balandin et al., 2008). The mechanical strength is reported to be in the range of 130 GPa, which is lower than that of pristine graphene but still significantly high compared to many other materials (Lee et al., 2008). Moreover, the optical transmittance was about 70-80% for a single layer, which was dependent on the degree of reduction and the thickness of the rGO film (Eda et al., 2010). Consequently, the increasing demand for good quality and large-scale production of graphene in engineering applications has necessitated the development of a facile and cost-effective methods for graphene synthesis. However, the expensive synthesis methods and small-scale production of graphene have hindered its industrial use, and as a result, focus has been channeled towards reduced graphene oxide (rGO), which has graphene-like properties. The incorporation of rGO into metal oxide (ZnO , MnO_2 , SnO_2 and TiO_2) composites capitalized on its active surfaces and exceptional carrier mobility, and demonstrably improved the performance and commercialization potential of diverse electronic devices (waveguides, solar cells, LEDs, phototransistors, lasers) (Liang et al., 2018; Lawal, 2019). Several methods have been used to synthesize rGO, including thermal reduction, hydrothermal method, and microwave irradiation (Tarcan et al., 2020) but these methods are not suitable for large-scale production and prevent practical application. Therefore, there is a growing demand and necessity for the production of rGO with a tunable energy band gap on a large scale.

Among the methods used to synthesize rGO, the chemical reduction of GO rich in oxygen functional groups synthesized from pristine graphite is a promising and practical method. GO has functional groups bonded in the basal plane (hydroxyl and epoxide groups to sp^3 carbons) and at the edges (carbonyl and carboxyl groups to sp^2 carbons). The active sites on the surface render GO hydrophilic (Wang et al., 2009). The chemical reduction facilitates the production of rGO on a large scale and at a low cost to meet various application requirements. Conventionally, hydrazine and hydrazine derivatives are used to deoxygenate GO but their corrosive, highly flammable and toxic nature hinder their economical use (Tene et al., 2020). The rGO prepared using these chemicals renders hydrophobic properties and leads to the agglomeration of rGO in solvents, which inhibits homogeneous dispersion.

To resolve the risks involved with reducing agents, research has been focused on finding effective and ecologically sound reducing agents for rGO synthesis. The search for alternative reducing agents has resulted in the introduction of numerous green reducers, such as aluminum, aqueous phyto extracts, baking soda, benzylamine, benzyl alcohol, beta carotene, caffeic acid, carrot root, casein, cinnamon, clove extract, coconut water, curcumin, *E. coli*, formic acid, *Ginkgo biloba*, grape juice, gallic acid, green tea polyphenol, glucosamine, glycine, *Hibiscus sabdariffa*, humanin, iron powder, L-ascorbic acid, L-cysteine, L-glutathione, L-lysine, L-valine, low temperature aluminum, melatonin, metallic zinc, metal salts, manganese powder, nascent hydrogen, natural cellulose +ionic liquid,

oligothiophene, oxalic acid, *Primula glutinosa*, PDDA, polyphenols, pomegranate juice, potassium, hydroxide, pyrrole, rose water, reducing sugar, spinach, *Shewanella* sp., sodium acetate trihydrate, sodium carbonate, sodium hydroxide, supercritical alcohols, *T. chebula*, tea solution, thiourea dioxide (TUD), tin powder, tannin, vitamin C, vitamin C+ amino acid and yeasts (Mahbubul et al., 2016).

In our study, GO was synthesized employing a modified version of the widely recognized Hummers method, tailored to reduce environmental impact through the use of safer reagents (Anuwongsa et al., 2023). The reduction of graphene oxide (GO) was carried out using an aqueous extract of *Chromolaena odorata* leaves. This process was validated through various characterization techniques. X-ray diffraction (XRD) analysis provided insights into the structural restoration of graphene, indicated by the reduced interlayer spacing in GO. Raman spectroscopy confirmed the removal of oxygen-containing groups and the reinstatement of the sp^2 carbon network, which is crucial for the structural integrity of reduced graphene oxide (rGO). The morphology and elemental composition of the synthesized rGO were examined using field emission scanning electron microscopy (FESEM) and energy dispersive x-ray spectroscopy (EDS), revealing a uniform and defect-free structure with minimal oxygen content. Fourier-transform infrared spectroscopy (FTIR) and Brunauer Emmet Teller (BET) analyses confirmed the reduction process, with a significant reduction in oxygen-related peaks and an increase in surface area and pore volume.

The primary reducing agent in the *Chromolaena odorata* extract was identified as flavonoids, which facilitated the reduction of GO. This research proposed an application for *Chromolaena odorata* and made a significant contribution to green chemistry in material synthesis. The successful demonstration of GO reduction using a plant extract highlighted the potential of natural resources in developing sustainable materials and paving the way for greener methodologies in graphene research.

2. Materials and Methods

2.1 Materials

Graphite powder (about 100 μm) was purchased from Union Science Trading Co., Ltd. Sulfuric acid (H_2SO_4 , 96%), sodium nitrate (NaNO_3 , 99%), potassium permanganate (KMnO_4 , 99%), hydrochloric acid (HCl, 37%), hydrogen peroxide (H_2O_2 , 30%) and ethanol ($\text{C}_2\text{H}_5\text{OH}$, 95%) were purchased from RCL Labscan and used as purchased. *Chromolaena odorata* plants were collected from the local area (Sakon Nakhon district, Thailand).

2.2 Preparation of GO powder

An eco-friendly adapted Hummers' method was opted for the synthesis of GO from pristine graphite powder over other chemical method (Anuwongsa et al., 2023).

1) High-purity graphite flakes from Union Science with the size of 140 mesh was ground to a fine powder using a ball mill (Retsch PM400). Graphite powder (15 g) was added in a flask of 250 mL volume and the particle size of the powder sample was then reduced by at least 20 μm using 25 grinding balls at 350 rpm for 30 min. Afterwards, the powder samples were sieved and shaken to obtain sample sizes of 90 microns. Finally, 10 g of graphite powder samples were added in the flasks of 12 mL volume and ground using 5 grinding balls at 350 rpm for 30 min.

2) A sample consisting of 10 g of graphite powder mixed with 10 g of NaNO_3 was added to 300 mL of H_2SO_4 in a conical flask. The mixture was stirred using a Velp AREC stirrer at 200 rpm for 30 min while soaking in an ice bath, maintaining the temperature at 0-5°C. To achieve controlled oxidation, a weight ratio of 1:3 was employed, where 30 g of KMnO_4 was added to 10 g of graphite (10 g graphite: 30 g KMnO_4).

Gradually introduced to the ice-cooled acidic mixture (maintained at ~0-5°C) to mitigate the exothermic reaction's abrupt temperature increase) and 300 mL of DI water was added and stirred by the agitator at 700 rpm. The mixture was allowed to respond for a period of 30 min. Then, 120 mL of H_2O_2 were added slowly with stirring at 700 rpm until a golden yellow color was obtained, which confirmed the termination of the oxidation.

3) The liquid graphite (golden yellow color) was diluted with 400 mL of DI water before being centrifuged (SUPER DEAL PRO 800) at 4000 rpm for 30 min and then filtered through Whatman Grade 5 filter paper to remove any undissolved particles. Thereafter, the mixture was ultrasonicated with a Branson ultrasonicator at 28 kHz for 6 h. Subsequently, 100 ml of HCl were then added and the mixture was stirred with a magnetic stirrer at 4,000 rpm for 30 min.

4) The GO was rinsed with deionized water until the pH changed to 7 before drying at 80°C for 8 h (Memmert, UNpa paraffin oven) to obtain the final sample of graphene oxide powder, as shown in Figure 1.

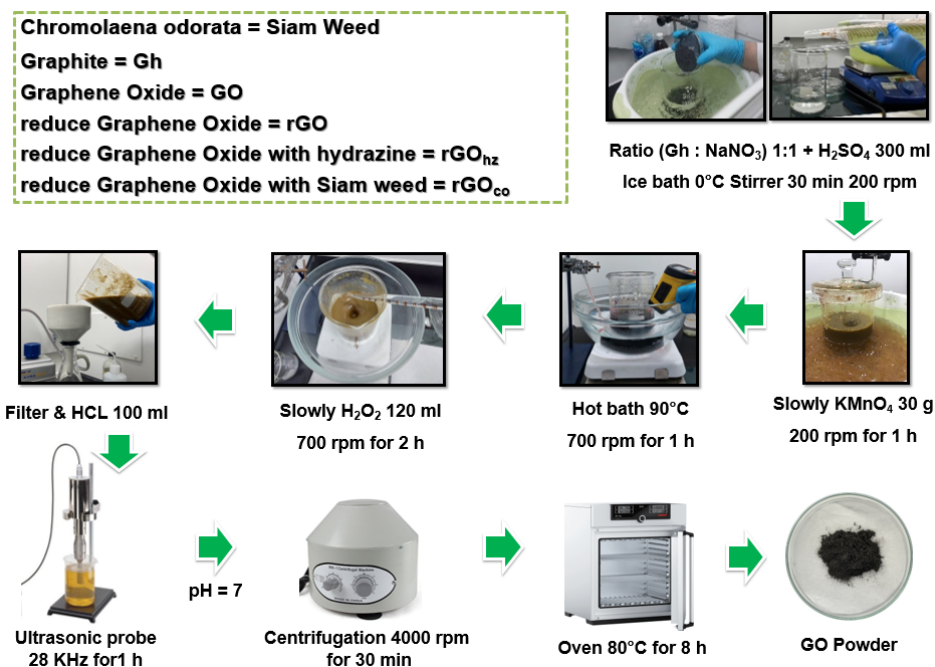


Figure 1. An illustration of the steps of the preparation of GO powder

2.3 Preparation of *Chromolaena odorata* extract

The leaves of *Chromolaena odorata* were washed with distilled water, cut into small pieces (500 g). These pieces were then added to 1500 mL of ethanol ($\text{C}_2\text{H}_5\text{OH}$) in a beaker. The

mixture was stirred continuously at 200 rpm for 30 min while maintaining a temperature of 80°C. After stirring, the mixture was subjected to vacuum evaporation at 45°C using a Velp AREC evaporator to remove excess ethanol. The extract was then cooled to room temperature and filtered with Whatman filter paper to remove solid residues. The filtered extract was stored at a temperature below 4°C until used for the reduction of GO.

2.4 Reduction of GO by *Chromolaena odorata* and hydrazine extract

The GO powder (0.02 mg) was added to a beaker containing *Chromolaena odorata* extract (10 mL) and exposed to an ultrasound probe for 2 h. The mixture was then stirred with a magnetic stirrer at 500 rpm. The stirring time and temperature were optimized to 40 h and 60°C to obtain rGO, which was indicated by a color change from brown to black (Figure 2). The resulting rGO was homogeneously dispersed in ethanol. For the reduction of GO by hydrazine extract (rGO_{hz}), the same procedure was followed, with replacement of the *Chromolaena odorata* extract with hydrazine extract.



Figure 2. Optical image of (a) GO, (b) rGO_{hz} and (c) rGO_{co}

2.5 Characterization techniques

The structural properties of GO and rGO were analyzed to determine their crystallinity and structure using X-ray diffraction (XRD) with a Shimadzu LabX XRD-6100. The chemical composition was identified through Raman spectroscopy (HORIBA Xplora plus). Different functional groups attached to GO and rGO were identified using a Thermo Fisher Scientific Fourier transform infrared (FTIR) spectrometer. The surface and internal structures, as well as the elemental composition, were examined using field emission scanning electron microscopy (FESEM) and energy dispersive x-ray spectroscopy (EDS) with a JEOL JSM-7610F. Additionally, the surface area and porosity were measured using the Brunauer-Emmett-Teller (BET) method with a MicrotracBEL BELSORP-miniX.

3. Results and Discussion

The x-ray diffraction (XRD) patterns in Figure 3 provide insights into the crystalline structure of graphite, graphene oxide (GO) and reduced graphene oxide (rGO) synthesized using two distinct reducing agents hydrazine (rGO_{hz}) and *Chromolaena odorata* extract (rGO_{co}). The sharp peak at ~26.07° in the graphite pattern reveals its well ordered structure with an interlayer spacing of 0.34 nm, characteristic of the (002) plane. This peak diminishes and shifts to a lower angle (12.56°) in the GO pattern, signifying an increase in interlayer spacing due to oxygen containing functional groups introduced during oxidation. The broadened peak shape further suggests the formation of defects and a decrease in

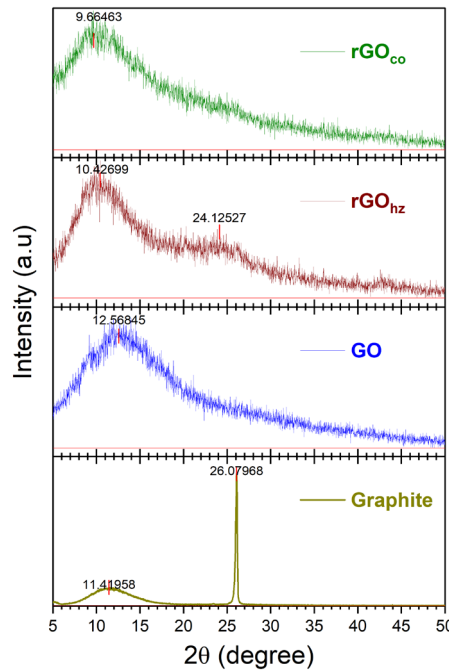


Figure 3. XRD patterns Graphite, GO, $r\text{GO}_{\text{hz}}$ and $r\text{GO}_{\text{co}}$

crystallinity. For the rGO samples, the peak positions shift towards higher angles compared to GO, signifying a partial restoration of the graphitic structure. The rGO synthesized using hydrazine ($r\text{GO}_{\text{hz}}$) displays a peak at 24.12° , which, while indicative of a decrease in interlayer spacing relative to GO, suggests that some oxygen functionalities remain, preventing a complete return to the structure of pristine graphite. In contrast, the rGO obtained from the eco-friendly *Chromolaena odorata* extract ($r\text{GO}_{\text{co}}$) exhibits a broad peak at 9.66° , which is significantly lower than that of $r\text{GO}_{\text{hz}}$. This unexpected shift could be attributed to the presence of different chemical environments or residual functional groups that were not fully removed during the reduction process. It may also suggest a higher degree of disorder or a larger interlayer spacing, possibly due to the insertion of biomolecules from the plant extract within the graphene layers. These observations indicate that while both reducing agents are effective in partially restoring the graphene structure from GO, there are distinct differences in the degree of reduction and the quality of rGO produced. The use of *Chromolaena odorata* extract as a green-reducing agent results in an rGO with unique structural properties compared to that from conventional hydrazine reduction, as evidenced by the shift in peak positions and the broader peak shapes in the XRD pattern. This study highlights the potential of using sustainable and environmentally friendly reducing agents such as plant extracts in the synthesis of graphene-based materials. However, the results also highlight the need for further optimization to improve the crystallinity and electrical properties of rGO to make it a viable replacement in applications typically dominated by materials reduced by traditional chemical methods.

The Raman spectra in Figure 4 provide a comparative analysis of the structural and electronic characteristics of commercial graphite, graphene oxide (GO), and reduced

graphene oxide (rGO) prepared through different methods. This powerful technique sheds light on the sp^2 -bonded carbon network, disorder, and electronic structure of these materials, offering valuable insights into their properties and potential applications. The Raman spectrum of pristine graphite is dominated by a sharp G peak at $\sim 1578\text{ cm}^{-1}$ (Figure 4(a)). This signature peak signifies the well-ordered sp^2 -bonded carbon network characteristic of the graphitic structure.

Upon oxidation to GO, a prominent D peak emerges at $\sim 1347\text{ cm}^{-1}$ (Figure 4(b)), reflecting the introduction of defects and disorder into the carbon lattice due to the presence of oxygen-containing functional groups. The G peak shifts to $\sim 1605\text{ cm}^{-1}$, indicating changes in the electronic structure and a decrease in the average size of the sp^2 domains. The broadening and reduced intensity of the 2D peak suggest the incorporation of functional groups, affecting the uniformity of the electronic band structure (E-k relation) in the measured area. The quantified ratio of D and G peak intensities (I_D / I_G) reaches ~ 1.00 , confirming the successful oxidation of graphite to GO and the significant presence of defects. The Raman spectrum of $r\text{GO}_{\text{hz}}$ reveals a D peak at $\sim 1359\text{ cm}^{-1}$ and a G peak at $\sim 1594\text{ cm}^{-1}$ (Figure 4(c)). While the position of the G peak suggests partial restoration of the sp^2 network, the I_D / I_G ratio of ~ 1.19 indicates a higher degree of disorder compared to GO. This discrepancy can be attributed to the aggressive nature of hydrazine, which likely introduces additional defects during the reduction process. Interestingly, the $r\text{GO}_{\text{co}}$ spectrum showcases a slightly lower I_D / I_G ratio of ~ 1.09 , implying fewer defects compared to $r\text{GO}_{\text{hz}}$ (Figure 4(d)). The D peak at $\sim 1342\text{ cm}^{-1}$ and the G peak at $\sim 1599\text{ cm}^{-1}$ suggest a partial restoration of the graphitic structure closer to pristine graphite. Although the 2D peak at $\sim 2685\text{ cm}^{-1}$ remains broad, it suggests fewer layers than GO, confirming the formation of rGO. These observations indicate that *Chromolaena odorata* extract acts as a gentler reducing agent, preserving more of the graphitic structure and introducing fewer defects compared to hydrazine. The lower I_D / I_G ratio and narrower G peak in the $r\text{GO}_{\text{co}}$ spectrum highlight the potential of plant extracts as sustainable and environmentally friendly alternatives for rGO production.

The L_a values were calculated using the equation:

$$L_a (\text{nm}) = \frac{(2.4 \times 10^{-10}) \lambda_l^4}{I_D / I_G}$$

Where λ_l is the laser line wavelength in nanometer units. This calculation method provides a quantifiable measure of the average crystallite size, allowing for the comparison of structural integrity across different samples. The data collectively indicate that *Chromolaena odorata* extract acts as a gentler reducing agent, preserving more of the graphitic structure and introducing fewer defects compared to hydrazine. This supports the potential of plant extracts as sustainable and environmentally friendly alternatives for the reduction of GO to rGO. The lower ratio and narrower G peak in the $r\text{GO}_{\text{co}}$ spectrum highlight the effectiveness of using plant extracts for high-quality rGO production, which could be beneficial for applications in electronic devices, energy storage, and composite materials.

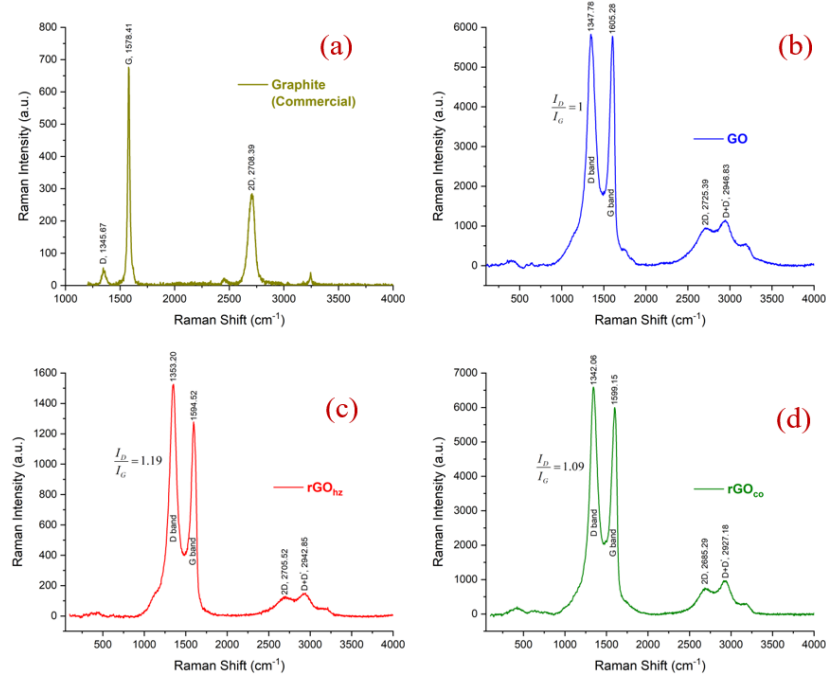


Figure 4. Raman spectra of (a) Graphite, (b) GO, (c) rGO_{hz} and (d) rGO_{co} .

The Raman spectra of Graphite, GO, rGO_{hz} , and rGO_{co} were analyzed, and the parameters are summarized in Table 1. Pristine graphite exhibits a remarkably low I_D / I_G ratio (0.08), indicative of minimal defects and a highly ordered sp^2 carbon structure. This is corroborated by its substantial crystallite size L_a of 240.31 nm, underscoring its well-preserved graphitic nature. The oxidation process significantly alters the material's structure, as evidenced by GO's markedly increased I_D / I_G ratio (1.00) and reduced L_a (19.22 nm). These changes reflect the introduction of numerous defects and structural disorders during oxidation. Subsequent reduction processes yield varying results. The rGO_{hz} displays a slightly higher I_D / I_G ratio (1.19) and further decreased L_a (16.16 nm), suggesting the introduction of additional defects during reduction. In contrast, rGO_{co} exhibits a lower I_D / I_G ratio (1.09) and larger L_a (17.64 nm) compared to rGO_{hz} , indicating a more preserved graphitic structure. The I_D / I_G ratio serves as a key indicator of disorder or defects in graphene materials, with higher values signifying increased defect density. Concurrently, the crystallite size (L_a) provides insight into the average dimensions of ordered domains within the samples.

These findings suggest that *Chromolaena odorata* extract functions as a milder reducing agent compared to hydrazine, resulting in fewer defects and larger crystallite sizes in the reduced graphene oxide. However, both reduction methods yield materials with more defects and smaller crystallite sizes than pristine graphite, highlighting the structural changes induced by the oxidation-reduction process.

Table 1. Parameters of Raman spectra for Graphite, GO, rGO_{hz} and rGO_{co}

Samples	D band (cm ⁻¹)	FWHM	G band (cm ⁻¹)	FWHM	I_D / I_G	L_a (nm)
Graphite	1346	23	1578	20	0.08	240.31
GO	1347	131	1605	65	1.00	19.22
rGO _{hz}	1353	121	1594	71	1.19	16.16
rGO _{co}	1342	123	1599	77	1.09	17.64

The FESEM image of pristine graphite (Figure 5(a)) depicts a uniform, smooth surface, highlighting its high crystallinity and layered structure. Sharp edges and a well-defined lattice pattern reflect the material's ordered nature. In contrast, the rGO images (Figure 5(b)) showcase a markedly different landscape. Wrinkles, folds, and fragmented edges dominate the rGO flake surfaces, a testament to the successful exfoliation and reduction processes. These features arise from the introduction of defects and the removal of oxygen containing functional groups during reduction. The higher magnification image (Figure 5(c-d)) further reveals the retained layered structure while emphasizing the enhanced surface roughness of rGO, a characteristic desirable for applications reliant on high surface area, such as energy storage and catalysis.

EDS analysis confirms the expected elemental composition changes between graphite and rGO. As shown in Table 2, the carbon content of graphite is high (96.23 At%), with a minimal oxygen presence (2.79 At%). Upon reduction, the carbon content in rGO increases, reflecting the removal of oxygen-containing functional groups. Oxygen reduction provides evidence of the effectiveness of the reduction process.

The combined FESEM and EDS analyses conclusively demonstrate the successful synthesis of rGO with a substantial reduction in oxygen content, confirming the effective removal of oxygenated functionalities from the precursor graphite oxide. The observed morphology of rGO, characterized by increased surface area and structural defects, suggests a material with promising potential for applications in various fields, particularly those benefiting from enhanced surface area and active sites, such as catalysis and energy storage.

Fourier-transform infrared (FTIR) spectroscopy sheds light on the vibrational characteristics of materials, offering valuable insights into the presence and type of functional groups present. In this study, FTIR analysis provides crucial evidence for the successful reduction of graphene oxide (GO) to reduced graphene oxide (rGO) using both conventional (hydrazine) and sustainable (*Chromolaena odorata* extract) methods. Figure 6 showcases the FTIR spectra of (a) pristine graphite, (b) GO, (c) rGO_{hz} (hydrazine reduced), and (d) rGO_{co} (*Chromolaena odorata* extract reduced). Each spectrum reveals distinct peak signatures, offering a fingerprint of the material's functional groups. Figure 6(a) with its nearly flat baseline signifies the minimal presence of functional groups in pure graphite, characterized by its sp²-hybridized carbon network. Figure 6(b), in stark contrast, shows the GO spectrum with a multitude of peaks indicative of diverse oxygen-containing functional groups introduced during oxidation. The broad peak around 3400 cm⁻¹ corresponds to O-H stretching vibrations, primarily from hydroxyl groups. Sharp peaks at ~1720 cm⁻¹ signify C=O stretching in carboxylic and carbonyl groups, while peaks around 1620 cm⁻¹ reflect residual un-oxidized graphitic regions with C=C stretching vibrations. Notably, peaks near 1050-1250 cm⁻¹ suggest the presence of epoxy and alkoxy groups, further confirming the extensive introduction of C-O functionalities. Figure 6(c) shows that

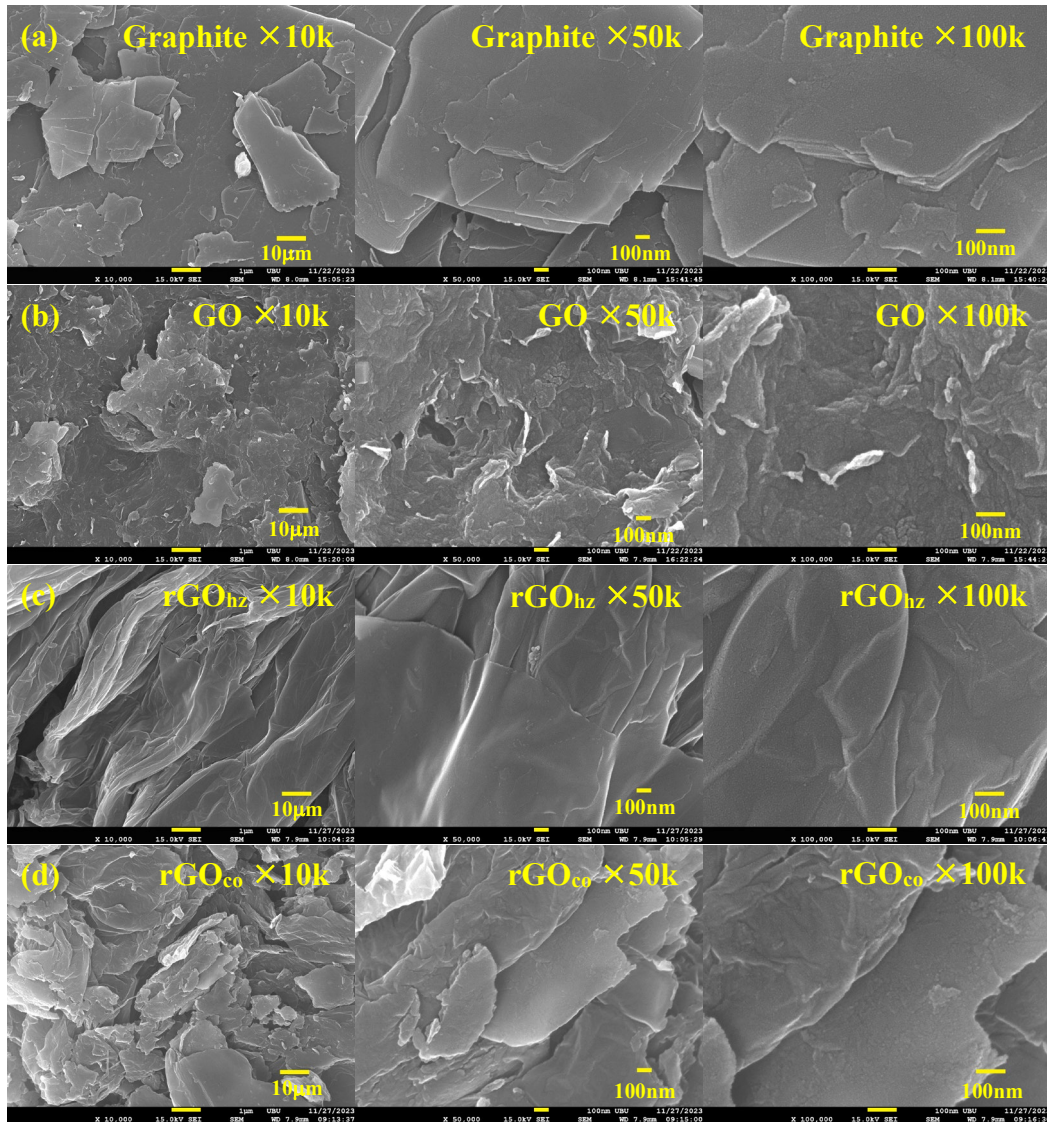


Figure 5. FESEM images of (a) Graphite, (b) GO, (c) rGO_{hz} and (d) rGO_{co}

Table 2. Elemental composition of Graphite, GO, rGO_{hz} and rGO_{co}

Samples	Carbon (At%)	Oxygen (At%)
Graphite	96.23	2.79
GO	67.26	27.21
rGO _{hz}	86.48	11.64
rGO _{co}	82.79	16.34

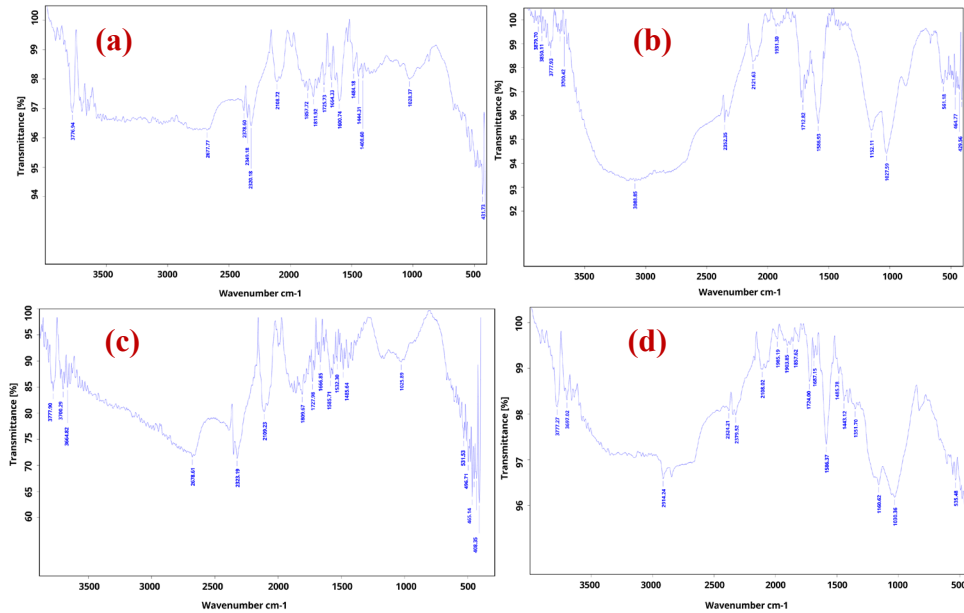


Figure 6. FTIR spectra of (a) Graphite, (b) GO, (c) rGO_{hz} and (d) rGO_{co}

while the rGO_{hz} spectrum exhibits decreased intensity in oxygen-related peaks compared to GO, indicating a partial reduction, residual peaks suggest incomplete removal of all functional groups. This is corroborated by the I_D / I_G ratio of 1.19, calculated from the peaks around 1620 cm^{-1} and 1720 cm^{-1} , which points to some disorder in the carbon lattice. Figure 6(d) showing the rGO_{co} spectrum highlights the effectiveness of *Chromolaena odorata* extract as a reducing agent.

Brunauer-Emmett-Teller (BET) analysis delves into the cryptic world of surface area and porosity, offering valuable insights into the structural properties of materials. In this study, BET sheds light on the transformations experienced by pristine graphite, graphene oxide (GO), and reduced graphene oxide (rGO) prepared with both conventional (hydrazine) and green (*Chromolaena odorata* extract) methods. Figure 7 showcases the nitrogen adsorption isotherms for Figure 7(a) graphite characterized by a low surface area of 4.3 $\text{m}^2 \text{ g}^{-1}$ and a predominantly microporous structure, as evidenced by the steep initial rise in the isotherm. Figure 7(b) GO: oxidation dramatically increases the surface area to 30.4 $\text{m}^2 \text{ g}^{-1}$ and introduces mesoporous features, attributed to the formation of oxygen containing functional groups, reflected by the hysteresis loop in the isotherm. Figure 7(c) rGO_{hz} partial restacking of the reduced sheets reduces the surface area to 6.4 $\text{m}^2 \text{ g}^{-1}$ compared to GO, but still higher than graphite. The isotherm shape suggests a blend of micropores and mesopores with an average pore diameter of 27.2 nm. Figure 7(d) rGO_{co}: promoting a higher surface area of 8.3 $\text{m}^2 \text{ g}^{-1}$ compared to both rGO_{hz} and GO. The open, less densely packed structure is evident from the isotherm and confirmed by the average pore diameter of 20.6 nm.

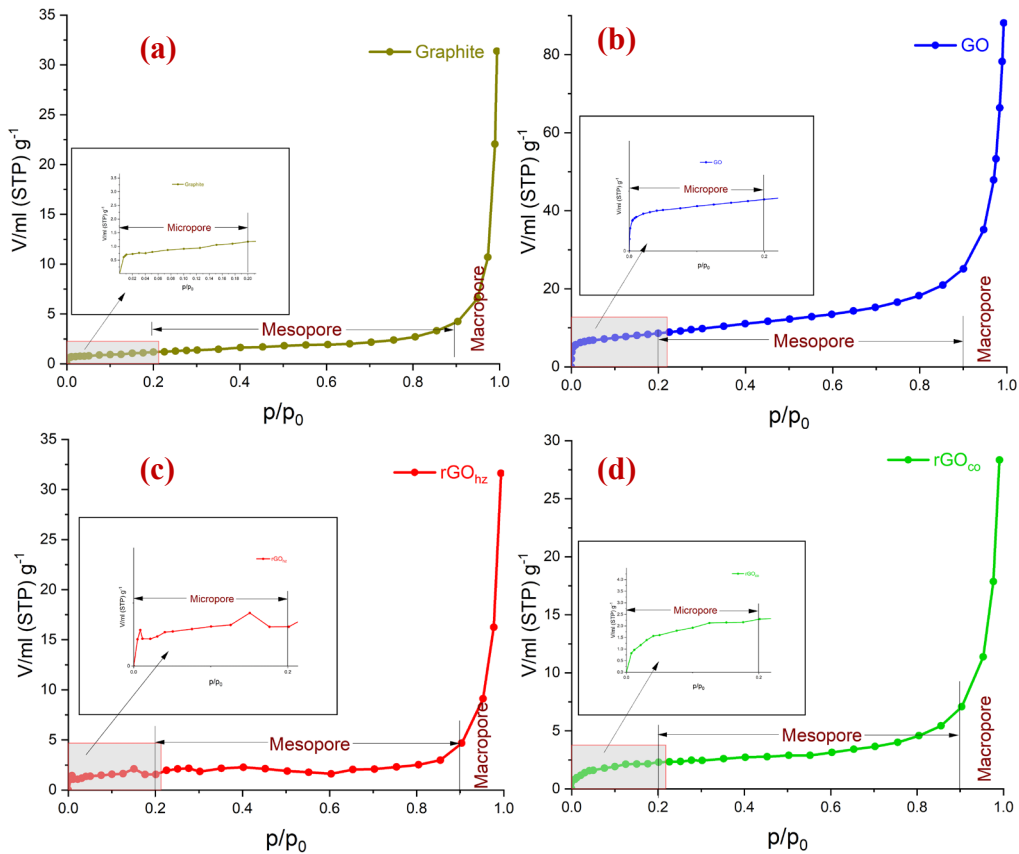


Figure 7. Brunauer Emmet Teller (BET) of (a) Graphite, (b) GO, (c) rGO_{hz} and (d) rGO_{co}

4. Conclusions

This study successfully demonstrates the use of *Chromolaena odorata* extract as an effective and eco-friendly reducing agent for synthesizing high-quality reduced graphene oxide (rGO). Our comprehensive analytical approach reveals several advantages of this green chemistry method. X-ray diffraction (XRD) analysis shows a decrease in interlayer spacing in rGO, indicating partial restoration of the pristine graphitic structure. Raman spectroscopy reveals a lower I_D / I_G ratio, implying fewer structural defects and a re-established sp² network. Field emission scanning electron microscopy (FESEM) images present a homogeneous rGO surface, further confirming successful reduction. Brunauer-Emmett-Teller (BET) analysis demonstrates a significant increase in rGO's surface area and pore volume compared to GO, highlighting the extract's effectiveness in maintaining an open and porous structure. Fourier-transform infrared spectroscopy (FTIR) spectra indicate a decrease in oxygen-related peaks, particularly a slight reduction at 1720 cm⁻¹, suggesting the removal of oxygen-containing functional groups from GO.

The use of *Chromolaena odorata* extract, an invasive weed and bio-waste, provides a sustainable alternative to conventional rGO production, reducing environmental impact and adding value to waste materials. The rGO produced via this method exhibits

an eco-friendly reducing agent for graphene oxide, making it suitable for various applications, including energy storage, sensing devices, and catalysis.

5. Acknowledgements

We would like to extend our gratitude to Thailand's Science Research and Innovation (TSRI) for their support of this work through the Fundamental Research Funds (grant No. 186275) provided to Rajabhat Sakon Nakhon University.

6. Conflicts of Interest

The authors declare no conflict of interest.

ORCID

Watsayod Ananpreechakorn  <https://orcid.org/0009-0005-1511-7556>
Krittaphat Wongma  <https://orcid.org/0009-0007-4719-0218>
Theerawut sumpao  <https://orcid.org/0009-0007-2993-2433>
Sunti Phewphong  <https://orcid.org/0000-0002-1666-3381>
Nattawat Anuwongsa  <https://orcid.org/0009-0001-1911-1304>
Hassakorn Wattanasarn  <https://orcid.org/0000-0001-6914-5935>

References

Alwan, S. H., Omran, A. A., Naser, D. K., & Ramadan, M. F. (2023). A mini-review on graphene: Exploration of synthesis methods and multifaceted properties. *Engineering Proceedings*, 59(1), Article 226. <https://doi.org/10.3390/engproc2023059226>

Anuwongsa, N., Yawai, T., & Ananpreechakorn, W. (2023). A simple preparation of graphene oxide with a modified Hummer's method. *Journal of Materials Science and Applied Energy*, 12(3), Article 251664. <https://doi.org/10.55674/jmsae.v12i3.251664>

Balandin, A. A., Ghosh, S., Bao, W., Calizo, I., Teweldebrhan, D., Miao, F., & Lau, C. N. (2008). Superior thermal conductivity of single-layer graphene. *Nano Letters*, 8(3), 902-907. <https://doi.org/10.1021/nl0731872>

Eda, G., Lin, Y.-Y., Mattevi, C., Yamaguchi, H., Chen, H.-A., Chen, I.-S., Chen, C.-W., & Chhowalla, M. (2010). Blue photoluminescence from chemically derived graphene oxide. *Advanced Materials*, 22(4), 505-509. <https://doi.org/10.1002/adma.200901996>

Lawal, A. T. (2019). Graphene-based nanocomposites and their applications: A review. *Biosensors and Bioelectronics*, 141, Article 111384. <https://doi.org/10.1016/j.bios.2019.111384>

Lee, C., Wei, X., Kysar, J. W., & Hone, J. (2008). Measurement of the elastic properties and intrinsic strength of monolayer graphene. *Science*, 321(5887), 385-388. <https://doi.org/10.1126/science.1157996>

Liang, F. X., Gao, Y., Xie, C., Tong, X. W., Li, Z. J., & Luo, L. B. (2018). Recent advances in the fabrication of graphene-ZnO heterojunctions for optoelectronic device applications. *Journal of Materials Chemistry C*, 6(17), 3815-3833. <https://doi.org/10.1039/C8TC00172C>

Mahbubul, M. T. H., Saidur, R., & Metselaar, H. S. C. (2016). The green reduction of graphene oxide. *RSC Advances*, 6, 27807-27828. <https://doi.org/10.1039/C6RA03189G>

Pei, S., Zhao, J., Du, J., Ren, W., & Cheng, H.-M. (2012). Direct reduction of graphene oxide films into highly conductive and flexible graphene films by hydrohalic acids. *Carbon*, 50(12), 3210-3215. <https://doi.org/10.1016/j.carbon.2010.08.006>

Tarcan, R., Todor-Boer, O., Petrovai, I., Leordean, C., Astilean, S., & Botiz, I. (2020). Reduced graphene oxide today. *Journal of Materials Chemistry C*, 8(4), 1198-1224. <https://doi.org/10.1039/C9TC04916A>

Tene, T., Tubon Usca, G., Guevara, M., Molina, R., Veltri, F., Arias, M., Caputi, L. S., & Vacacela Gomez, C. (2020). Toward large-scale production of oxidized graphene. *Nanomaterials*, 10(2), Article 279. <https://doi.org/10.3390/nano10020279>

Wang, G. X., Shen, X. P., Wang, B., Yao, J., & Park, J. (2009). Synthesis and characterisation of hydrophilic and organophilic graphene nanosheets. *Carbon*, 47, 1359-1364. <https://doi.org/10.1016/j.carbon.2009.01.027>

Zhu, Y., Murali, S., Cai, W., Li, X., Suk, J. W., Potts, J. R., & Ruoff, R. S. (2010). Graphene and graphene oxide: Synthesis, properties, and applications. *Advanced Materials*, 22(35), 3906-3924. <https://doi.org/10.1002/adma.201001068>